Solid State Phenomena Vol. 215 (2014) pp 409-414
Online available since 2014/Apr/11 at www.scientific.net

doi:10.4028/www.scientific.net/SSP.215.409

Domain structures in films with combined magnetic anisotropy. Two-dimensional simulation.

M.N. Dubovik[a,1,2], V.V. Zverev[2], B.N. Filippov[1,2]

[1] Institute of Metal Physics, UB RAS, S. Kovalevskoy str. 18, Yekaterinburg 620990, Russia

[2] Ural Federal University, Mira str. 19, Yekaterinburg 620002, Russia

[a]e-mail: dubovik@imp.uran.ru

Keywords: micromagnetic simulations, tetra-axial anisotropy, domain walls, domain structures.

Abstract. The domain structure dependence on the uniaxial anisotropy constant has been considered in a micrometer-thick film by means of the two-dimensional micromagnetic simulation. The film has both uniaxial and tetra-axial magnetic anisotropies. The new type domain structures and walls caused by the tetra-axial anisotropy presence are predicted.

Introduction

Magnetic anisotropy type and magnitude are among the key factors determining the sample domain structure. In films with the easy axis directed normally to the film surface and $Q = \sqrt{K / 2\pi M_S^2} > 1$ (K – the anisotropy constant, M_S – the saturation magnetization) the open structure exists. In such a structure the domains magnetization is directed strictly outwards the film plane, with twisted domain walls [1] separating the domains. At $Q < 1$ the closed structure arises with the magnetic flux closed in the film body thus decreasing magnetostatic energy. With a succeeding decrease in K the magnetization **M** lies in the film plane [2]. In this work the transition between the structures mentioned has been investigated in detail with making allowance for tetra-axial anisotropy. Such anisotropy exists in yttrium iron garnet and nickel films as the crystallographic one (the uniaxial perpendicular anisotropy is usually available as the induced one). New types of domain structures have been predicted at the certain ratio of the uniaxial and tetra-axial anisotropy constants. Those structures containing 109º and 90º vortex-like domain walls are fairly new as no vortex-like walls of that type were known before.

Statement of the problem

The micromagnetic simulations were performed using OOMMF [3]. A film fragment under consideration had the dimensions L_x=6000 nm, L_y=1000 nm (the film thickness), $L_z \to \infty$. The latter approximation was implemented using periodic boundary conditions [4], with the magnetization being treated as a function of two coordinates: $\frac{\mathbf{M}}{M_S} = \mathbf{m}(x, y)$. The equilibrium domain structure was obtained by minimizing the total energy of the sample per unit length along the z axis:

$$E = \int_0^{Lx} \int_0^{Ly} \left(f_e + f_m + f_a \right) dxdy \,, \tag{1}$$

$$f_e = A\left\{ \left(\frac{\partial \mathbf{m}}{\partial x} \right)^2 + \left(\frac{\partial \mathbf{m}}{\partial y} \right)^2 \right\}, \quad f_m = -\frac{1}{2} M_s \mathbf{m}\mathbf{H}^{(m)},$$

$$f_a = K_u \left(m_x^2 + m_y^2 \right) + K_1 \left(\frac{1}{4} m_x^4 + \frac{1}{3} m_y^4 + \frac{1}{4} m_z^4 - \frac{\sqrt{2}}{3} \sin 3\varphi\, m_x^3 m_y + \frac{\sqrt{2}}{3} \cos 3\varphi\, m_y m_z^3 + \right.$$

$$\left. + \frac{1}{2} m_x^2 m_z^2 - \sqrt{2} \cos 3\varphi\, m_x^2 m_y m_z + \sqrt{2} \sin 3\varphi\, m_x m_y m_z^2 \right),$$

where A is the exchange parameter; $\mathbf{H}^{(m)}$ is the magnetostatic field obtained by solving the equations of magnetostatics with the usual boundary conditions; K_u is the uniaxial anisotropy constant; K_1 is the tetra-axial anisotropy constant; φ is the angle between the z axis and the crystallographic direction $[11\bar{2}]$ (see Fig. 1). The expression for the tetra-axial anisotropy contribution is obtained by the transformation from the coordinate system related to the crystallographic axes [100], [010], and [001] (components with the tilde) to the coordinate system related to the film geometry (components without the tilde). In the coordinate system related to the crystallographic axes, the tetra-axial anisotropy energy density has the standard form $K_1\left(m_x^2 m_y^2 + m_y^2 m_z^2 + m_z^2 m_x^2\right)$, $K_1 < 0$. Further, if not stated otherwise, we will use the coordinate system related to the film geometry (Fig. 1) and restrict ourselves to the case $\varphi = 0$. $A = 4.15 \cdot 10^{-7}$ erg/cm, $M_S = 140$ G, $K_1 = -6500$ erg/cm^3 (yttrium iron garnet parameters).The quantity K_u was varied in the range from $2 \cdot 10^5$ erg/cm^3 to zero with a minimum step of 1000 erg/cm^3. For every nonzero value of K_u, we compared the results of calculations performed with or without the tetra-axial anisotropy ($K_1 = 0$). The calculations were performed using a rectangular mesh of uniformly magnetized cells. The cell size was 5 nm that did not exceed both the stray field exchange length and the wall width parameter for the material parameters considered.

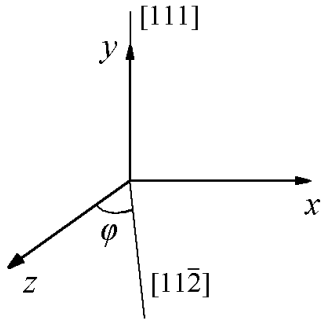

Fig. 1. *Orientation of the crystallographic directions and coordinate axes.*

Results and discussions

Fig. 2*(a)* shows the equilibrium magnetization distribution corresponding to the case of uniaxial anisotropy prevalence. That is the open structure with conventional twisted domain walls. Let's denote d_m the domain structure period corresponding to the minimum of (1). The plot d_m vs K_u is shown in figure 2*(b)*. Let the uniaxial anisotropy constant decreases, beginning with $K_u = 2 \cdot 10^5$ erg/cm^3. Initially, the d_m value slightly decreases too. That is accounted for by a domain wall energy lowering that provides a way to decrease the magnetostatic energy due to the partition of the film into a larger number of domains. Then, however, the period d_m begins to increase rapidly due to qualitative changes in the character of the **m** distribution in the computational region. As the uniaxial anisotropy constant K_u decreases, the magnetization in domains starts deviating from the easy axis direction near the film surfaces, thus decreasing the density of magnetostatic poles on these surfaces. The regions with deviated **m** enlarge and the tilting angle increases with a further decrease in K_u. Withal the domain walls expand along the x axis and the period d_m increases. As a result the closed structure illustrated in fig. 3 arises. This structure resembles the Landau–Lifshitz one but have some peculiarities. Let's use the scheme shown in fig. 3*(b)* for explanation. The domain walls thicknesses here cannot be considered to be small with respect to the size of domains. In the vicinity of the lines *AB* and *DE*, there are twisted domain walls with a two-dimensional structure and the lines *BC*, *CD*, *EF*, and *FA* can be considered as 90º domain walls. At the points *C*, C_1, C_2, *F*, F_1, and F_2, the **m** direction is collinear with the direction of the z axis. The lowest energy is observed in the structure in which the magnetization directions in all lines of the *AB* type and at points of the *C* and *F* types coincide. In such a case the exchange energy is lower than the exchange

energy corresponding to the alternating **m** directions in the above-mentioned regions. It is clear, however, that the circumstances may change with making allowance for the finite size L_z.

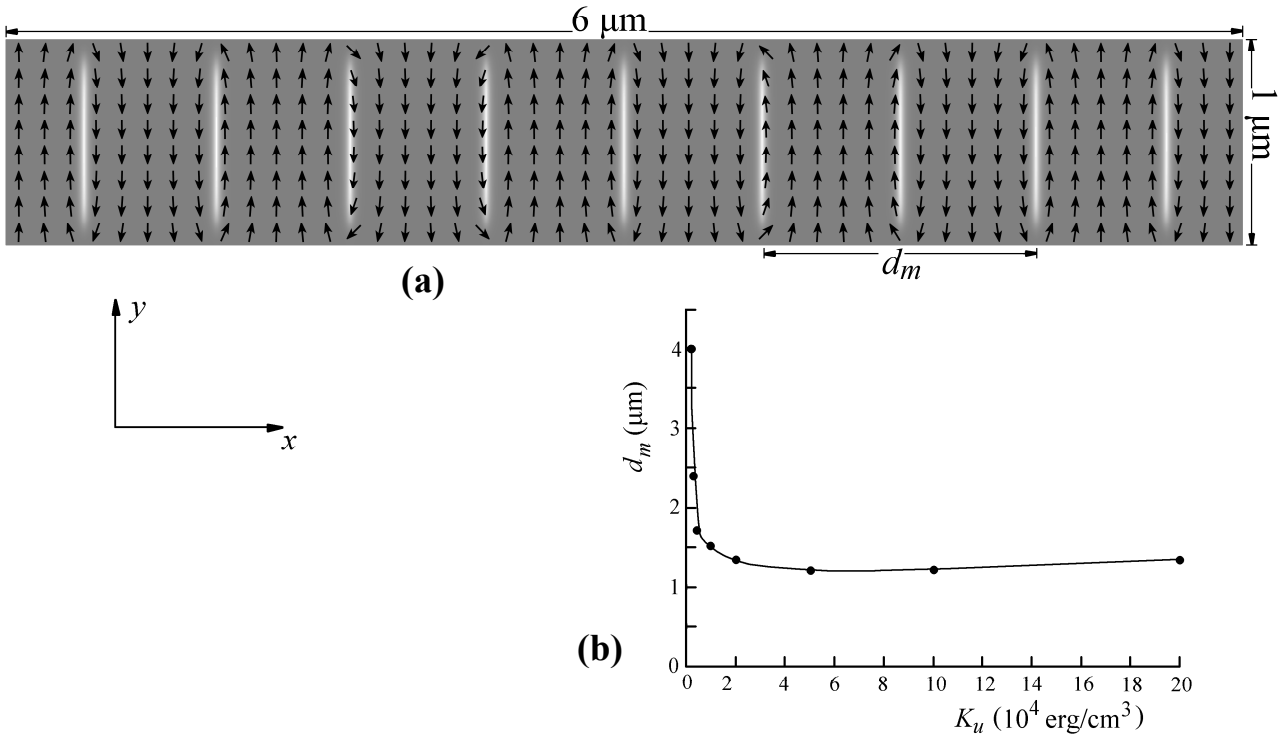

Fig. 2. *(a). Complete equilibrium distribution of the magnetization in the xy plane for $K_u = 2 \cdot 10^5$ erg/cm^3. Transition from the white background to the grey one corresponds to m_z varying from -1 to 0. (b) Dependence of the period of the domain structure with the minimal energy on the uniaxial anisotropy constant.*

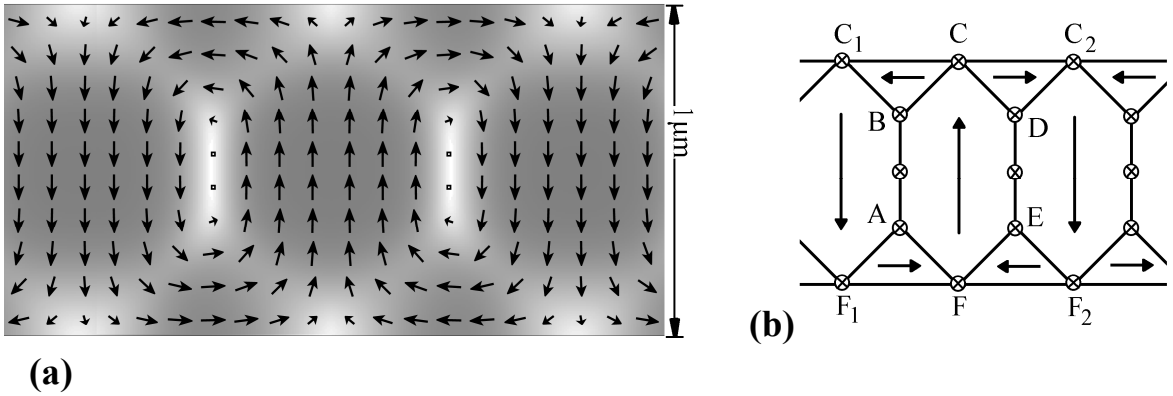

Fig. 3. *(a). Fragment of the equilibrium magnetization distribution in the xy plane for $K_u = 10^4$ erg/cm^3. Transition form the white background to the grey one corresponds to the change from $m_z = -1$ to $m_z = 0$. (b) Schematic illustration of the equilibrium distribution of the magnetization in the xy plane.*

The tetra-axial magnetic anisotropy at the chosen ratio of K_1 and K_u does not play a decisive role in the formation of the structures shown in Fig. 2, 3. It was verified by the calculations performed for $K_1 = 0$ with the fixed other parameters. But at $K_u \leq 3000$ erg/cm^3 the tetra-axial anisotropy starts to effect on the equilibrium **m** distribution essentially. The corresponding domain structure and its schematic diagram are shown in fig. 4. Now, in the central part of the film, there are alternating

domains with **m**(0, 1, 0) and with $\mathbf{m}(0,-\frac{1}{3},-\frac{2\sqrt{2}}{3})$, represented in the diagram by regions of the types *ABCD* and CEA_1F, respectively, with the regions of the types *BCE* and *DCF* closing the magnetic flux. This distribution of the magnetization **m** significantly decreases the magnetostatic energy of the sample at the sufficiently low total magnetic anisotropy energy because the direction $\mathbf{m}(0,-\frac{1}{3},-\frac{2\sqrt{2}}{3})$ is parallel to the crystallographic direction [111] (the one of the easy axes corresponding to the tetra-axial anisotropy). Like for the structures discussed above, the lowest energy is observed when the **m** directions at all *A*, *B*, *C*, *D*, *E*, and *F* points coincide (turn our attention once again to the fact that this result relates to $L_z \to \infty$).

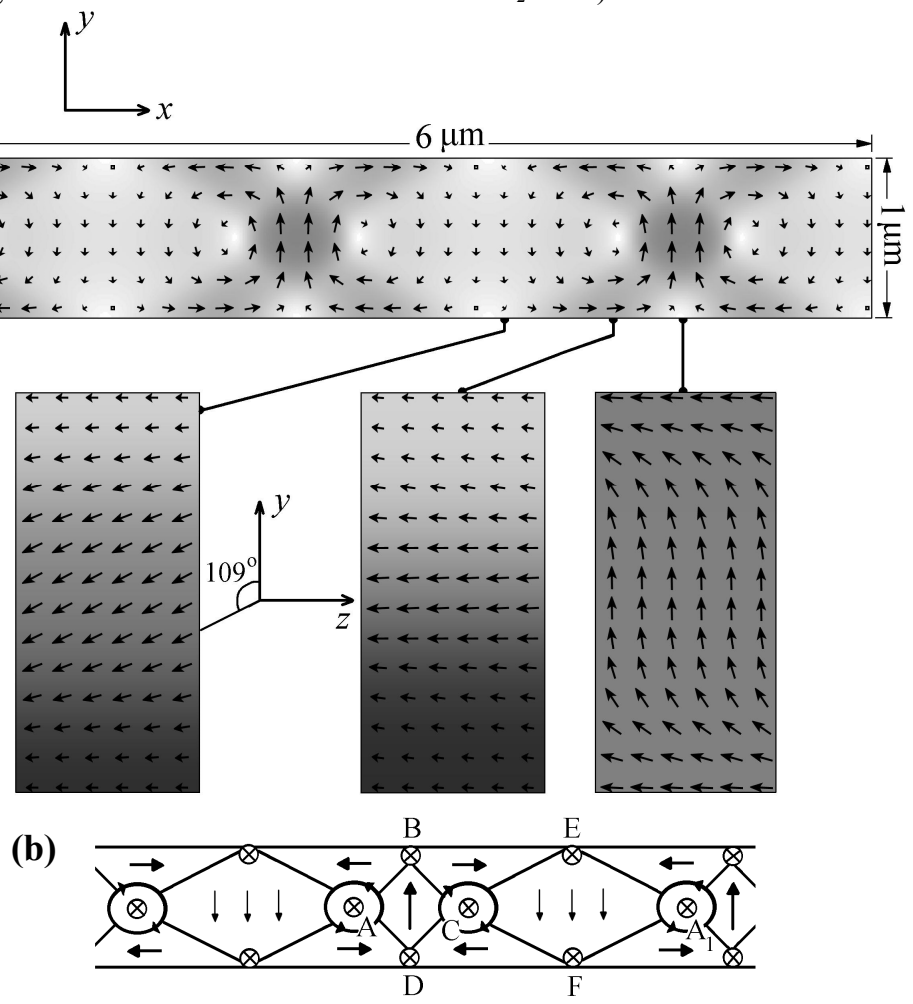

Fig. 4. *(a). Complete equilibrium distribution of the magnetization in the xy plane and its cross-sections in the yz plane for K_u = 3000 erg/cm^3. Transition from the white background to the grey one corresponds to m_z varying from -1 to 0 for the xy plane; transition from the white background to the black one corresponds to m_x varying from -1 to +1 for the yz plane. (b) Schematic illustration of the magnetization distribution in the xy plane.*

The sizes of the *ABCD* type and CEA_1F type domains are different. Near the points *B*, *E*, *D*, and *F*, the magnetization is oriented collinear to the direction of the *z* axis. The angle between this direction and the direction of the magnetization **m** for the *ABCD* region is greater than that for the CEA_1F region. Therefore, ∇m_i and div**m** (and, hence, the densities of the exchange and magnetostatic energies) grow more rapidly as approaching the film surface in the *ABCD* region. That's why its smaller size is energetically favorable.

The domain walls separating the regions *ABCD* and CEA_1F are novel 109º vortex-like walls. The vortex core polarization in such a wall depends on the **m** orientation in the neighboring domains. In the case illustrated in fig. 4, at the points *A*, *C*, and A_1, the magnetization can be directed only against the direction of the *z* axis. A similar structure with the opposite polarization (in the aforementioned points the magnetization **m** has the direction of the *z* axis) will separate domains with **m**(0, –1, 0) and $\mathbf{m}(0,\frac{1}{3},\frac{2\sqrt{2}}{3})$. It has been found that the domain structure illustrated in Fig. 4 is stable with respect to small perturbations in the angle φ in the vicinity of zero. It must be noted also that the scheme shown in fig. 4*(b)* is only a simplified diagram, which facilitates perception. Actually the magnetization varies smoothly, so that **m** has the exact directions of the easy axes only in the middle part of the regions *ABCD* and CEA_1F.

With a further decrease in K_u domains of the CEA_1F type extend and their magnetizations smoothly rotate from the $(0,-\frac{1}{3},-\frac{2\sqrt{2}}{3})$ direction to the $(0,0,-1)$ direction. Thus the 109º vortex-like domain walls turn into the 90º vortex-like ones at K_u=2000 erg/cm^3 (see fig. 5). This intermediate structure exists before the predominant **m** orientation in the film plane is achieved at K_u=1000 erg/cm^3. This result is in a good agreement with the analytical expression for the thickness D_c of stripe domains nucleation in a zero magnetic field: $D_c = 2\pi\sqrt{\frac{A}{K_u}}$ [2]. This formula gives the value close enough to L_y at the corresponding K_u magnitude.

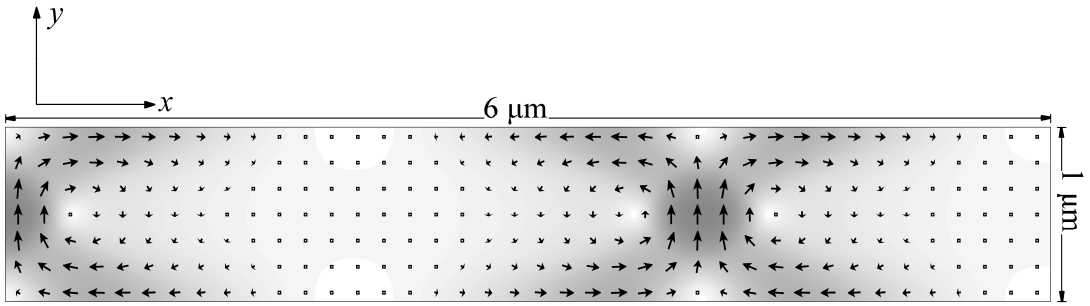

Fig. 4. *Complete equilibrium magnetization distribution in the xy plane for K_u = 2000 erg/cm^3. Transition from the white background to the grey one corresponds to the change from m_z = –1 to m_z = 0.*

In the case K_1=0 the transformation from the structure illustrated by fig. 3 to the in-plane magnetized film comes by the other way. In this case the structures with 109º and 90º domain walls are unstable. As a decrease in the uniaxial anisotropy constant progresses, the domain structure undergoes the following changes: the period d_m slightly increases, the relative sizes of regions of the types BC_1C and AFF_1 (see fig. 3) increase, the domain walls extend along the *x* axis, and the magnetization in the regions of the *ABCDE* type (fig. 3) begins to deviate gradually from the direction of the *y* axis. As a result, domains and domain walls in this structure have very close characteristic sizes, so that the mental separation of these elements becomes difficult (see [5] for the details). At K_u=1000 erg/cm^3 the in-plane **m** orientation becomes energetically favorable like in the case with $K_1 \neq 0$.

Conclusions

The transformation from the open domain structure to the closed one with a decrease in the uniaxial anisotropy constant has been investigated. This transformation is accompanied by penetrating the twisted walls Néel sections in films with $Q > 1$ into the domain region, thus

eliminating the magnetostatic poles in the open structure. The transition from the closed structure to the in-plane magnetized film is influenced by the crystallographic tetra-axial anisotropy that leads to formation of domain structures with the domains of different sizes separated by the 109º and 90º vortex-like domain walls.

Acknowledgements

This work was supported by the Russian Foundation for Basic Research (project no. 11-02-00931) and the Department of the Physical Sciences of the Russian Academy of Sciences (program no. 12-T-2-1007).

References

[1] E.Schlomann, J. Appl. Phys. 44 (1973) 1837.

[2] A. Hubert, IEEE Trans. Magn. 21 (1985) 1605.

[3] M. J. Donahue and D. G. Porter, OOMMF User's Guide: Version 1.0, NISTIR 6376 (National Institute of Standards and Technology, Gaithersburg, Maryland, 1999).

[4] K. M. Lebecki, M. J. Donahue, M. W. Gutowski, J. Phys. D. 41 (2008) 175005.

[5] M. N. Dubovik, V. V. Zverev, B. N. Filippov, Phys. Solid State 55 (2013) 2057.

Trends in Magnetism: Nanomagnetism (EASTMAG-2013)
10.4028/www.scientific.net/SSP.215

Domain Structures in Films with Combined Magnetic Anisotropy. Two-Dimensional Simulation
10.4028/www.scientific.net/SSP.215.409